ACS OMEGA

http://pubs.acs.org/journal/acsodf Article

A Combined Algorithm Using Both the MINLP Model and Approximated MILP Model for PVC Production Scheduling

Jian Su, Yuhong Wang,* and Xiaoyong Gao

Cite This: *ACS Omega* 2022, 7, 26047−26055

Read Online

ABSTRACT: In this paper, a scheduling model of PVC production by a calcium carbide method is designed based on a continuous-time modeling method, and an improved mixed-integer nonlinear programming (MINLP) model for scheduling of PVC production is proposed. The optimization goal is to minimize the total cost. Considering the practical requirements of both the solution rapidity and quality, a combined algorithm is further established using both the MINLP model and approximated mixed-integer linear program (MILP) model for PVC production scheduling. The optimization result of the linear model is substituted into the original MINLP model as the initial value of variables to accelerate the solution process. Then, the optimal solution of the improved model is executed. Afterward, the effectiveness of the proposed method is verified with two actual cases. The comparative results demonstrate that the proposed algorithm can significantly accelerate the computation and obtain more accurate optimal solution.

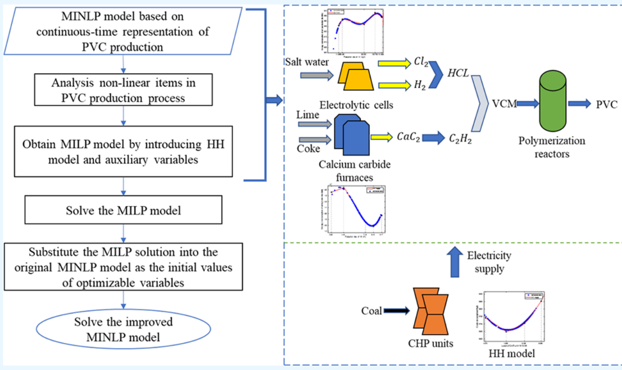

1. INTRODUCTION

Polyvinyl chloride (PVC) is a common plastic widely used in various fields such as industry and agriculture. The calcium carbide method is primarily employed to produce PVC in China due to the abundance of coal and the lack of petroleum resources, whose capacity accounts for over 81%. The substantial energy consumption has provided strong motivation for optimal operation of PVC plants, and plant-wide scheduling optimization has become an attractive option. In our previous work, the multiperiod planning optimization model of a PVC plant was established,[1] and the original MINLP model was linearized to an approximated MILP model by introducing the hinging hyperplanes (HH) model to accelerate the solution.[2] However, the optimization result based on the HH model is an approximate solution, which can hardly meet the need of high-precision scenes in industry. Additionally, it is inevitable for the discrete-time based model to increase the number of scheduling periods to acquire a more accurate scheduling solution, which would lead to a larger scale model and more computational time. The efficient solution remains challenging due to the intrinsic nonlinearities of the process and current modeling approaches.

There are abundant related research results on the scheduling optimization problem modeling and solving of PVC production. Tian et al. studied the scheduling problem of PVC production and proposed an MILP model based on the discrete-time modeling method,[3,4] then the method of pinch point analysis was introduced to optimize equipment variables,[5] and the layered optimization strategy was further proposed to accelerate the solution.[6] Wang et al. established an optimization model for the whole process planning of PVC production based on the discrete-time modeling method.[1] Gao et al. introduced the planning optimization model based on piecewise linear approximation, and the nonlinear characteristics in the actual production were linearized by fragments to avoid nonlinear problems in the modeling process,[2] which reduced the scale of the model and greatly accelerated the solution. With the purpose of handling the shortcomings of discrete-time modeling method, the continuous-time modeling method is capturing more attention.[7−9] González-González et al. proposed a multi-objective model for the forest harvest scheduling problem in the continuous-time framework.[10] Christian et al. proposed a hydrothermal scheduling model in the continuous-time framework.[11] Feleke et al. presented an extended graphical genetic algorithm for scheduling of gasoline production and distribution.[12]

With respect to MINLP problems, there are many research reports. Jaffal et al. presented a K-best branch and bound technique for the MINLP problem, which decreases the

Received: February 12, 2022
Accepted: July 11, 2022
Published: July 21, 2022

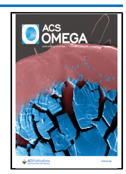

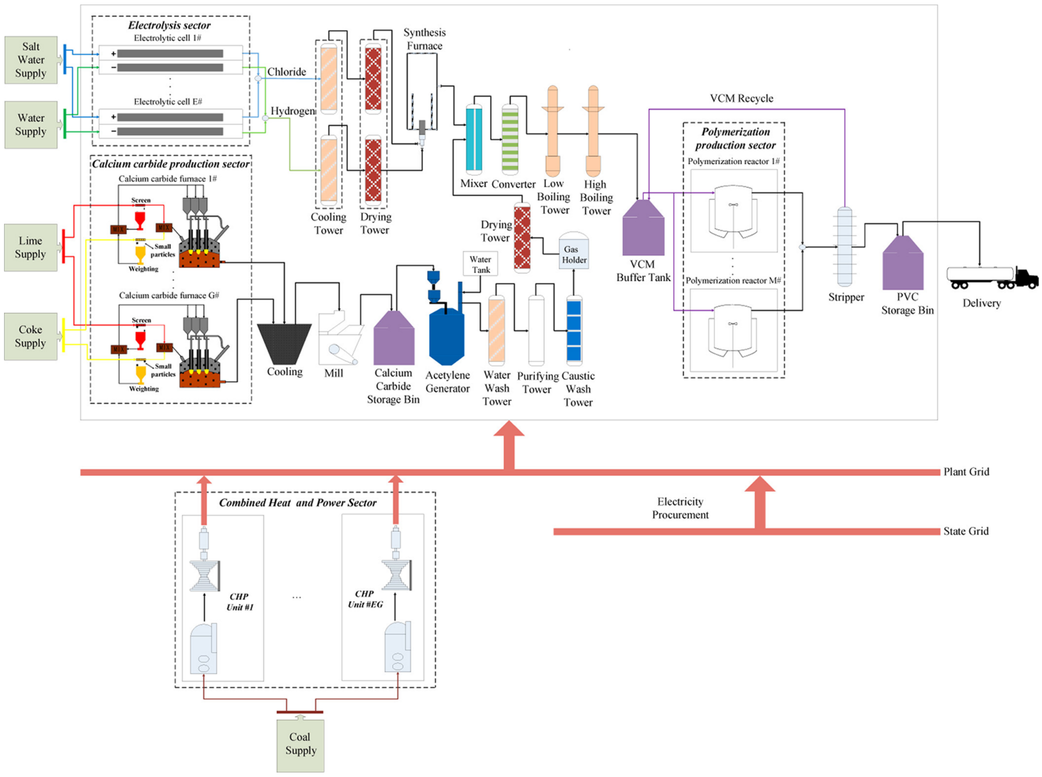

Figure 1. PVC production process.[1]

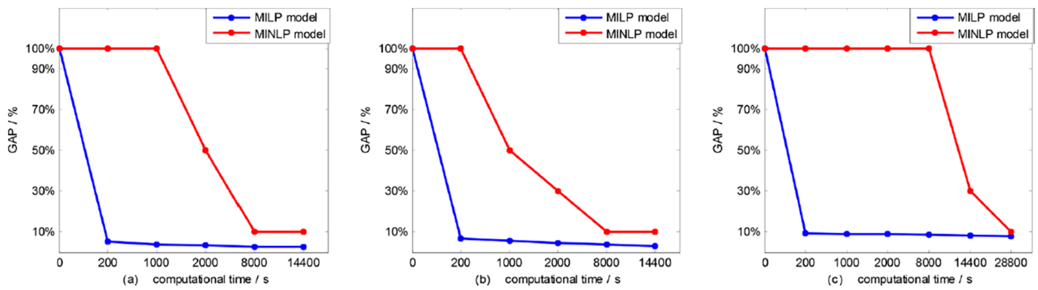

Figure 2. Comparison of convergence rates of models in PVC industrial cases varying sizes (a) case 1, (b) case 2, and (c) case 3.[2]

computational complexity.[13] Xiang et al. proposed a gradient-based algorithm for non-smooth constrained optimization problems governed by discrete-time nonlinear equations.[14] Jodie and Michael proposed parameterizations of data-driven nonlinear dynamic process models for fast scheduling calculations, the data-driven Hammerstein−Wiener models were applied to represent the dynamics of process variables, which reduced the size of the scheduling optimization problem.[15] Despite this valuable progress on MINLP solving, due to the large scale of industrial PVC scheduling problem, its unsatisfying convergence speed is also the main obstacle for industrial use.

Given the above problem, an MINLP model for the whole process scheduling of PVC production is established based on the continuous-time modeling method. Then, the linearization of the complex nonlinear problems is performed to accelerate the solution of the production scheduling problem. On this basis, the approximate optimal solution obtained by the MILP model based on the piecewise linear approximation is adopted as the initial values of variables in the original MINLP model to quickly obtain the optimization result. Moreover, the effectiveness of the proposed algorithm is verified using two actual cases.

The rest of this paper is organized as follows. The process description and the problem statement are provided in Section 2. In Section 3, the mathematical model based on continuous-time representation is established. In Section 4, the improved MINLP model is proposed. Afterward, the feasibility of the improved MINLP model is verified with a case study in Section 5. Finally, conclusions are drawn in Section 6.

2. PROBLEM STATEMENT

The whole process of PVC production is investigated in this paper with the domestic typical PVC production process by the calcium carbide method, as illustrated in Figure 1. There are two systems in the picture: a power supply system and material processing system.[6] The supply of electricity in the power supply system comes from the CHP units and the state grid. The material processing system consists of two production processes: vinyl chloride (VCM) production and synthesis of PVC by VCM polymerization.[16] VCM is synthesized from raw materials such as saltwater, coal, and lime. It is stored in storage tanks and then transported to the polymerization reactors. In addition, different grades of PVC products are obtained under different reaction conditions.

Both the material processing system and the utility system contain a large number of parallel equipment, such as electrolytic cells, calcium carbide furnaces, storage tanks, polymerization reactors, and CHP units. According to the actual industrial data collected, most of the production equipment possesses non-linear characteristics. Although the direct solution of the MINLP model can achieve good accuracy, the application speed in actual production is too slow. In addition, though the solution of the MILP model based on piecewise linear approximation can close the optimality gap rapidly compared with the original MINLP model, which has been verified by three cases of PVC production scheduling in our previous work in Figure 2, the accuracy can hardly meet the need of high-precision scenes due to the intrinsic error of the linearized model. Thus, the combined method is proposed, and the initial solution obtained by the linear approximation MILP model is substituted into the MINLP model for further optimal solution to meet the practical requirements of both the solution rapidity and quality.

Additionally, the mathematical model of the scheduling optimization problem of PVC production is established, and the combined algorithm is employed to solve. Finally, resource consumption and various costs are reduced, and the rapidity and quality of the solution are guaranteed. The scheduling optimization model is detailed in the next chapter.

3. PROBLEM FORMULATION

3.1. Time and Product Switching Constraint.

(1) Time constraint: equation 1 reveals that there is a minimum time interval between two different operations on one device. w indicates the event point within the scheduling period, $T_{\min}$ represents the minimum time interval between two adjacent event points, and $w_{\max}$ denotes the maximum number of w.

$$T_{w-1} + T_{\min} \le T_w, \quad 2 \le w \le w_{\max} \tag{1}$$

The time T_1 at which the first event occurred must be greater than the minimum time interval $T_{\min}$, as illustrated in eq 2.

$$T_1 \ge T_{\min} \tag{2}$$

(2) Switch constraints: (1) Product switching process. $y^s_{u,i,i',w} = 1$ suggests that the product in polymerization reactor u begins to switch from i to i' at the event w; $y^e_{u,i,i',w} = 1$ represents the end of product switching of the polymerization reactor u. Only one start and end action of product switching will occur at the same event point (eq 3). The beginning and end of the product switching process should orderly alternate for each equipment (eq 4).

$$\sum_i \sum_{i'} y^s_{u,i,i',w} + \sum_i \sum_{i'} y^e_{u,i,i',w} \le 2 \quad \forall\, u \in M,\, i \in MP,\, i' \in MP,\, i \ne i', w \in W \tag{3}$$

$$0 \le \sum_{k \le w} \sum_i \sum_{i'} y^s_{u,i,i',w} - \sum_{k \le w} \sum_i \sum_{i'} y^e_{u,i,i',w} \le 1 \quad \forall\, u \in M,\, i \in MP,\, i' \in MP,\, i \ne i', w \in W \tag{4}$$

(2) Steady-state production process. The binary variable $\omega_{u,i,w}$ indicates that the polymerization reactor u is in a steady-state production at the event w. At the two adjacent time points, one device has the same operating modes, as demonstrated in eq 5.

$$\omega_{u,i,w} + \omega_{u,i',w+1} \le 1 \quad \forall\, u \in M,\, i \ne i', w \le W \tag{5}$$

If the polymerization reactor u is in a product switching process in event w , then $\sum_i \omega_{u,i,w} = 0$; if the polymerization reactor u is in a steady-state process in event w, then $\sum_i \omega_{u,i,w} = 1$. The relationship between switching and steady processes is shown in eq 6.

$$\sum_{k \le w} \sum_i \sum_{i'} y^s_{u,i,i',w} - \sum_{k \le w} \sum_i \sum_{i'} y^e_{u,i,i',w} \le 1 - \sum_i \omega_{u,i,w+1} \quad \forall\, u \in M,\, i \in MP,\, w \in W \tag{6}$$

3.2. Material Processing Constraint.

(1) PVC polymerization process: According to market demand and inventory restrictions,[17] the yield of the PVC product i in the polymerization reactor u is $PT_{u,i,w}$. The polymerization process is a batch process, and the feed flow rate of the stable operation mode is $sFS_{u,i,w}$. The constraints are provided in eq 7.

$$PT_{u,i,w} = sFS_{u,i,w} \times \alpha_{u,i} \quad \forall\, u \in M,\, i \in MP,\, w \in W \tag{7}$$

The inventory constraints of different grades of PVC products are expressed in eqs 8 and 9. The current PVC stock $MI_{i,w}$ is equal to the stock at the previous moment $MI_{i,w-1}$ plus the production volume $PT_{u,i,w}$ and then minus the delivery volume $S_{i,w}$. The inventory of PVC product i is bounded between minimum inventory MI_i^{min} and maximum inventory MI_i^{max}.

$$MI_{i,w} = MI_{i,w-1} + \sum_{u \in M} PT_{u,i,w} - S_{i,w} \quad \forall\, i \in MP,\, w \in W \tag{8}$$

$$MI_i^{min} \le MI_{i,w} \le MI_i^{max} \quad \forall\, i \in MP,\, w \in W \tag{9}$$

(2) VCM production process: According to the production process of PVC, the corresponding consumption of VCM is expressed in eq 10. As illustrated in Figure 1, hydrogen chloride reacts with acetylene to obtain VCM. Following the strict chemical reaction equilibrium equation, the relationship between VCM, hydrogen chloride, and acetylene is expressed in eqs 11 and 12. The inventory constraints of VCM are expressed in eqs 13 and 14.

$$CM_{vcm,w} = \sum_{u \in M} \sum_{i \in MP} sFS_{u,i,w} \quad \forall\, w \in W \tag{10}$$

$$PT_{vcm,w} = CM_{Hcl,w} + CM_{C_2H_2,w} \quad \forall\, w \in W \tag{11}$$

$$\frac{CM_{Hcl,w}}{36.5} = \frac{CM_{C_2H_2,w}}{26} \quad \forall\, w \in W \tag{12}$$

$$MI_{vcm,w} = MI_{vcm,w-1} + PT_{vcm,w} - CM_{vcm,w} \quad \forall\, w \in W \tag{13}$$

$$MI_{vcm}^{min} \le MI_{vcm,w} \le MI_{vcm}^{max} \quad \forall\, w \in W \tag{14}$$

https://doi.org/10.1021/acsomega.2c00875
ACS Omega 2022, 7, 26047−26055

(3) Chlorine production process: The production of chlorine is the primary step of the PVC production process, and the yield is related to the working state $Z_{u,w}$, production time $T_{cl_2,u,w}$, and production rate of the electrolytic cells $P_{cl_2,u,w}$, as expressed in eq 15. In actual plants, the rate of chlorine production should be limited to a reasonable range, and $P_{cl2,u,w}$ is restricted by eq 16. Since the production process of chlorine is continuous and the stock is limited, the production of chlorine is consistent with the consumption of chlorine, as presented in eq 17.

$$PT_{cl2,u,w} = Z_{u,w} \times P_{cl2,u,w} \times T_{cl2,u,w} \quad \forall\ u \in E,\ w \in W \tag{15}$$

$$P^{min}_{cl2,u} \times Z_{u,w} \leq P_{cl2,u,w} \leq P^{max}_{cl2,u} \times Z_{u,w} \quad \forall\ u \in E,\ w \in W \tag{16}$$

$$\sum_{u \in U} PT_{cl2,u,w} = CM_{cl2,w} \quad \forall\ u \in E,\ w \in W \tag{17}$$

$P^{max}_{cl_2,u}$ indicates the maximum production rate of chlorine in the electrolytic cell. The production process of calcium carbide can be considered a continuous process. The relationship among the output of calcium carbide, the working state of calcium carbide furnace, production rate, and production time is expressed in eq 18. The production rate limit of the calcium carbide furnaces is presented in eq 19. Additionally, the inventory constraints of calcium carbide are shown in eqs 20 and 21.

$$PT_{cac2,u,w} = Z_{u,w} \times P_{cac2,u,w} \times T_{cac2,u,w} \quad \forall\ u \in G,\ w \in W \tag{18}$$

$$P^{min}_{cac2,u} \times Z_{u,w} \leq P_{cac2,u,w} \leq P^{max}_{cac2,u} \times Z_{u,w} \quad \forall\ u \in G,\ w \in W \tag{19}$$

$$MI_{cac2,w} = MI_{cac2,w-1} + \sum_{u \in G} PT_{cac2,u,w} - CM_{cac2,w} \quad \forall\ u \in G,\ w \in W \tag{20}$$

$$MI^{min}_{cac2} \leq MI_{cac2,w} \leq MI^{max}_{cac2} \quad \forall\ w \in W \tag{21}$$

(4) Calcium carbide production process: Hydrogen chloride is obtained through the reaction of chlorine and hydrogen, and acetylene is obtained through the reaction of calcium carbide and water. The reaction process of hydrogen chloride and acetylene can be considered complete and ideal. Therefore, the production of hydrogen chloride and acetylene is proportional to the consumption of chlorine gas and calcium carbide, respectively. In actual production, the capacity of the gas cabinet for storing acetylene gas is small, and the storage of acetylene is negligible. Accordingly, the yield of acetylene is considered equal to the consumption of acetylene, as expressed in eqs 22–24.

$$CM_{Hcl,w} = \gamma \times CM_{cl2,w} \quad \forall\ w \in W \tag{22}$$

$$PT_{C2H2,w} = \beta \times CM_{cac2,w} \quad \forall\ w \in W \tag{23}$$

$$PT_{C2H2,w} = CM_{C2H2,w} \quad \forall\ w \in W \tag{24}$$

where γ represents the relationship between the production of hydrogen chloride and the consumption of chlorine and β denotes the relationship between the production of acetylene and the consumption of calcium carbide.

(5) Energy constraint: The power consumption of calcium carbide furnaces and electrolytic cells is the main source of energy consumption in the whole plant. Figure 3 demonstrates a strong nonlinear relationship between power consumption and the production rate of calcium carbide and chlorine. The power consumption characteristics of different calcium carbide furnaces are different. The relationship between power consumption and production rate can be obtained by polynomial fitting. $f_u(P_{cl2,u,w})$ and $f_u(P_{cac2,u,w})$ represent the mathematical relationship between power consumption and the production rate of calcium carbide and chlorine, respectively. Therefore, the total power consumption of the calcium carbide furnace and the electrolytic cell is presented in eq 25:

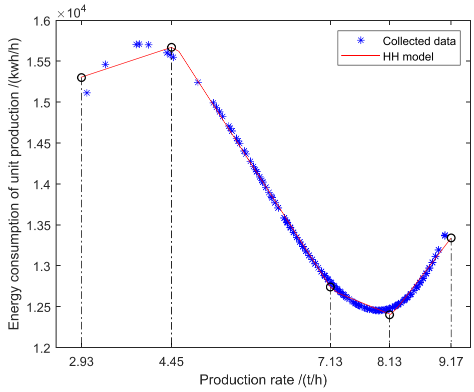

Figure 3. HH model for a calcium carbide furnace electricity consumption.

$$ele_w = \sum_{u \in E} f_u(P_{cl2,u,w}) \times PT_{cl2,u,w} + \sum_{u \in G} f_u(P_{cac2,u,w}) \times PT_{cac2,u,w} \quad \forall\ w \in W \tag{25}$$

where $PT_{cl2,u,w}$ and $PT_{cac2,u,w}$ indicate the production of chlorine and calcium carbide, respectively.

The supply of electricity comes from CHP units $PE_{u,w}$ and the state grid SG_w, as expressed in eq 26. To meet the demand for power consumption, the power supply $elesp_w$ should meet eq 27. Finally, the relationship among the power supply amount $PE_{u,w}$ of the CHP unit, the unit operating state $Z_{u,w}$, the power $Pw_{u,w}$, and the running time $T_{CHP,u,w}$ is provided in eq 28. Meanwhile, the constraint of the power supply capability of the CHP unit is presented in eq 29.

$$elesp_w = \sum_{u \in EG} PE_{u,w} + SG_w \quad \forall\ w \in W \tag{26}$$

$$elesp_w \geq ele_w \quad \forall\ w \in W \tag{27}$$

$$PE_{u,w} = Z_{u,w} \times Pw_{u,w} \times T_{CHP,u,w} \ \forall\ u \in EG \tag{28}$$

https://doi.org/10.1021/acsomega.2c00875
ACS Omega 2022, 7, 26047−26055

$$Z_{u,w} \times Pw_{u,w}^{min} \leq Pw_{u,w} \leq Pw_{u,w}^{max} \times Z_{u,w} \quad \forall\ u \in EG,\ w \in W \tag{29}$$

3.3. Objective Function. The objective is to minimize the overall cost, as revealed in eq 30. The total cost is composed of the cost of raw material (coke, coal, salt, and limestone) (eq 31), the out-of-stock penalty (eq 32), the cost of inventory (PVC inventory, VCM inventory, calcium carbide inventory, and raw material inventory) (eq 33), start-stop and product switching penalty (eq 34), and power consumption (eq 35).

$$cost = C_1 + C_2 + C_3 + C_4 + C_5 \tag{30}$$

$$C_1 = \sum_{r \in MR} \sum_{w \in W} CRM_r \times SP_{r,w} \tag{31}$$

$$C_2 = \sum_{i \in MP} \sum_{w \in W} Py_i \times (D_{i,w} - S_{i,w}) \tag{32}$$

$$C_3 = CI_i \sum_{w \in W} \sum_{i \in MP} MI_{i,w} + CI_r \sum_{w \in W} \sum_{r} MI_{r,w} + CI_{vcm} \sum_{w \in W} MI_{vcm,w} + CI_{cac2} \sum_{w \in W} MI_{cac2,w} \tag{33}$$

$$C_4 = \sum_{u \in M} \sum_{w \in W} CF_u \times ZF_{u,w} + \sum_{u \in M} \sum_{i \in MP} \sum_{w \in W} (1 - \omega_{u,i,w}) \cdot topCot \tag{34}$$

$$C_5 = CE \times \sum_{w \in W} SG_w \tag{35}$$

where CRM_r represents the price of the raw material r; Py_i indicates the penalty factor of the shortage of the PVC product i; CI_i, CI_r, CI_{vcm}, and CI_{cac2} denote the inventory price of the PVC product i, the stock price of the raw material r, the stock price of the VCM, and the stock price of the calcium carbide, respectively; CF_u refers to the start-stop switching price of the device u; $topCot$ signifies the operating cost when the product model is converted; CE indicates the electricity price of the state grid.

4. IMPROVED MINLP MODEL

Considering the practical requirement of computing speed and precision, a combined algorithm is established using both the MINLP model and approximated MILP model for PVC production scheduling. First, the nonlinearity of constraints such as eq 15 is simplified based on the method proposed by You and Grossmann.[18] Two auxiliary variables $ZP_{cl2,\ u,\ w}$ and $AX_{cl2,\ u,\ w}$ are introduced, and eq 15 can be replaced with eqs 36−40. Equations 18 and 28 are handled using the same method.

$$PT_{cl2,u,w} = ZP_{cl2,u,w} \times T_{cl2,u,w} \quad \forall\ u \in E,\ w \in W \tag{36}$$

$$ZP_{cl2,u,w} + AX_{cl2,u,w} = P_{cl2,u,w} \quad \forall\ u \in E,\ w \in W \tag{37}$$

$$ZP_{cl2,u,w} \leq Z_{u,w} \times P_{cl2,u}^{max} \quad \forall\ u \in E,\ w \in W \tag{38}$$

$$AX_{cl2,u,w} \leq (1 - Z_{u,w}) \times P_{cl2,u}^{max} \quad \forall\ u \in E,\ w \in W \tag{39}$$

$$ZP_{cl2,u,w} \geq 0,\ AX_{cl2,u,w} \geq 0 \quad \forall\ u \in E,\ w \in W \tag{40}$$

Due to the intrinsic nonlinearities of power consumption of equipment, the superiority of the piecewise linear (PWL) technique in dealing with nonlinear problems is considered.[19,20] Then, the PWL based on the HH model is introduced to approximate the complex nonlinear term in the original MINLP model, making the model linear locally while nonlinear globally. The general form of the sliced linear function used in this paper is presented in eq 41:

$$f(x|\theta) = x^T\theta_0 + \sum_{i=1}^{M} c_i max(0,\ x^T\theta_i) \tag{41}$$

where x denotes a vector with the first element of 1, namely, $x = [1,\ x_1,\ ...,\ x_n]^T$; θ represents a parameter vector of an odd function; M, θ_i, and c_i are the number of linked hyperplanes, the parameter vector of the ith hinge function, and the linear coefficient of the ith basis function, respectively.

The model expressed by eq 42 is applied to approximate the nonlinear function. Assuming that the nonlinear function is $y(x)$, the required parameters can be determined by eq 41 through the gradient method and the least-squares method:

$$V_N(\theta) = \frac{1}{2} \sum_{i=1}^{N} (y_i - f(x_i|\theta))^2 \tag{42}$$

where y_i indicates the output of the corresponding input of the nonlinear function, $\theta = [\theta_0,\ \theta_1,\ \cdots,\ \theta_M]^T$.

equation 42 is minimized as eq 43:

$$minV_N(\theta) = \frac{1}{2} \sum_{i=1}^{N} (y_i - f(x_i|\theta))^2 \tag{43}$$

According to the above method, all parameters of the HH model can be obtained based on data training. An improved MILP model is established by embedding the trained HH model into the original MINLP model. The total power consumption expressed in eq 25 can be transformed into the PWL expression in eq 44.

$$elesp_w = \sum_{u \in E} F_u(P_{cl2,u,w}) \times Z_{u,w} \times T_{cl2,u,w} + \sum_{u \in G} F_u(P_{cac2,u,w}) \times Z_{u,w} \times T_{cac2,u,w} \quad \forall\ w \in W \tag{44}$$

where F_u indicates the piecewise linear function approximated by the HH model to the nonlinear function $f_u \times P_{u,\ w}$. The HH models for the electricity consumption of a calcium carbide furnace and an electrolytic cell are illustrated in Figures 3 and 4. Additionally, the same processing method of the CHP unit in the power supply system is applied, and the result is presented in Figure 5.

However, the obtained result is an approximate solution since the MILP model is a linear approximation of the original model. Therefore, the results acquired by the linear model are substituted into the original MINLP model as the initial variables to generate the optimal solution of the model. The procedure of the improved MINLP model is exhibited in Figure 6.

Specifically, the initial value of optimizable variables such as start-stop switch variables of the equipment and the production rate of chlorine, calcium carbide, and VCM in each period can be obtained by the MILP model. Meanwhile, the consumption of intermediate products can also be obtained with the material constraints in the scheduling model. Then, the initialization of the improved MINLP model is achieved by setting the initial values of optimizable variables. Finally, the costs and operational

https://doi.org/10.1021/acsomega.2c00875
ACS Omega 2022, 7, 26047−26055

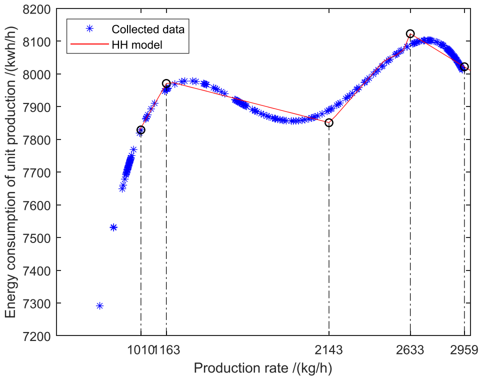

Figure 4. HH model for an electrolytic cell electricity consumption.

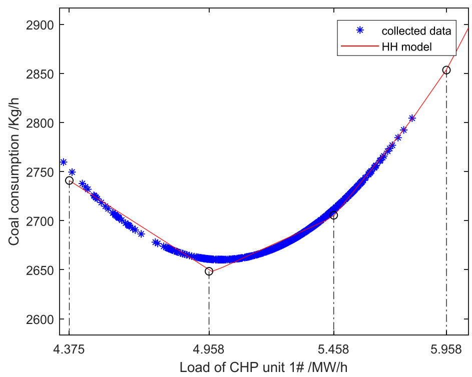

Figure 5. HH model for a CHP unit coal consumption.

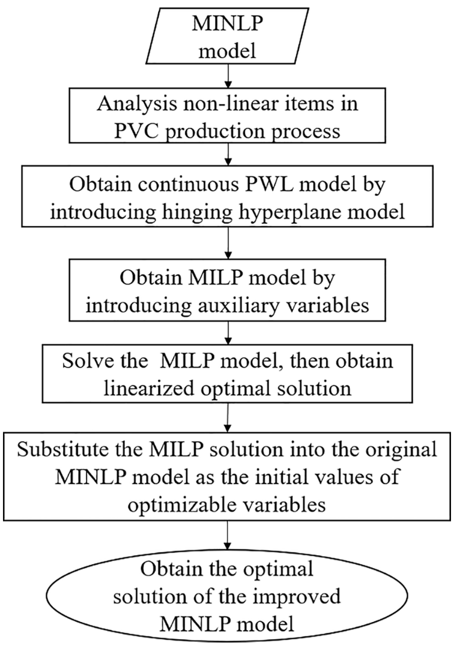

Figure 6. Procedure of the improved MINLP model.

variables such as production rate of the equipment are optimized more precisely by the improved MINLP model.

5. RESULTS AND DISCUSSION

To demonstrate the effectiveness of the improved MINLP model, two industrial cases are provided in this section. These cases both originate from a real-world PVC plant that includes 8 polymerization reactors, 8 calcium carbide furnaces, and 10 electrolytic cells. All cases are tested by GAMS win 32 24.0.2 and solved by Alpha-ECP in an Intel Core i5 CPU, 3.1GHz machine with 8GB of RAM based on the win10 operating system.

Table 1 shows the demands of five different PVC products and the delivery time in the future of 168 h. Moreover, a larger industrial case is provided to further verify the performance of the improved model, which considers a 336 h scheduling period, and the demands are shown in Table 2.

Table 1. Demands of Case 1

		products/t				
order	delivery time/h	A	B	C	D	E
1	24	140	130	100	230	100
2	36	140	140	120	150	100
3	60	120	130	100	250	260
4	108	100	300	150	220	140
5	120	250	120	145	185	130
6	144	245	155	230	100	100
7	168	140	300	365	220	100

Table 2. Demands of Case 2

		products/t				
order	delivery time/h	A	B	C	D	E
1	24	120	85	100	240	100
2	36	0	60	220	160	120
3	60	45	130	0	140	235
4	108	145	0	65	150	240
5	120	0	240	80	285	80
6	144	245	80	90	0	100
7	168	320	100	120	150	180
8	192	220	50	0	65	150
9	204	120	110	120	0	55
10	252	0	160	130	140	320
11	276	170	130	150	0	65
12	288	245	235	140	70	75
13	312	285	0	145	160	35
14	336	125	65	0	245	230

The statistics of the models are manifested in Table 3. Clearly, the scale of the MINLP model based on the continuous-time modeling method (MINLP II) is smaller than the model based on the discrete-time modeling method (MINLP I), since there are fewer events of the continuous-time modeling method. Meanwhile, the scale of the improved MINLP model (MINLP

Table 3. Model Statistics

	models	event number	constraint number	continuous variables	discrete variables
case 1	MINLP I	28	29,402	13,398	13,440
	MILP	7	7868	2569	4060
	MINLP II	7	8104	4445	3360
	MINLP III	7	8104	4445	3234
case 2	MINLP I	56	59,054	26,950	26,880
	MILP	14	15,785	5131	8120
	MINLP II	14	16,497	8883	6720
	MINLP III	14	16,497	8883	6468

https://doi.org/10.1021/acsomega.2c00875
ACS Omega 2022, 7, 26047−26055

Table 4. Objective Value and Computational Time in Different Optimality Gaps

	model	cost/CNY	absolute difference/CNY	relative value	CPU time/s	relative CPU time	gap
case 1	MINLP II	6,287,170			493		0.5
	MINLP III	6,123,520	163,650	2.6%↓	16	96.8%↓	0.5
	MINLP II	5,931,667			1266		0.2
	MINLP III	5,927,907	3760	0.6%↓	1741	37.5%↑	0.2
case 2	MINLP II	10,786,300			578		0.5
	MINLP III	10,312,490	179,200	1.7%↓	159	72.5%↓	0.5
	MINLP II	9,089,375			2314		0.3
	MINLP III	8,876,247	213,128	2.3%↓	593	74.4%↓	0.3

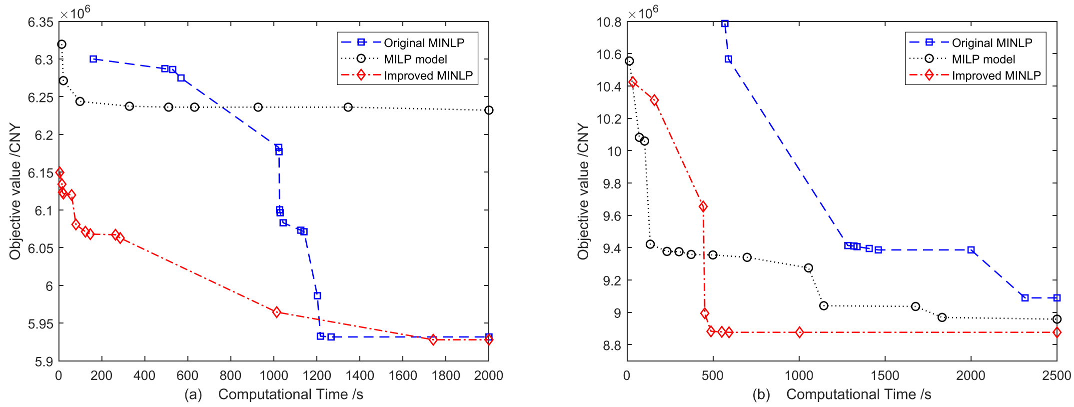

Figure 7. Relationship between the objective value and the computational time for (a) case 1 and (b) case 2.

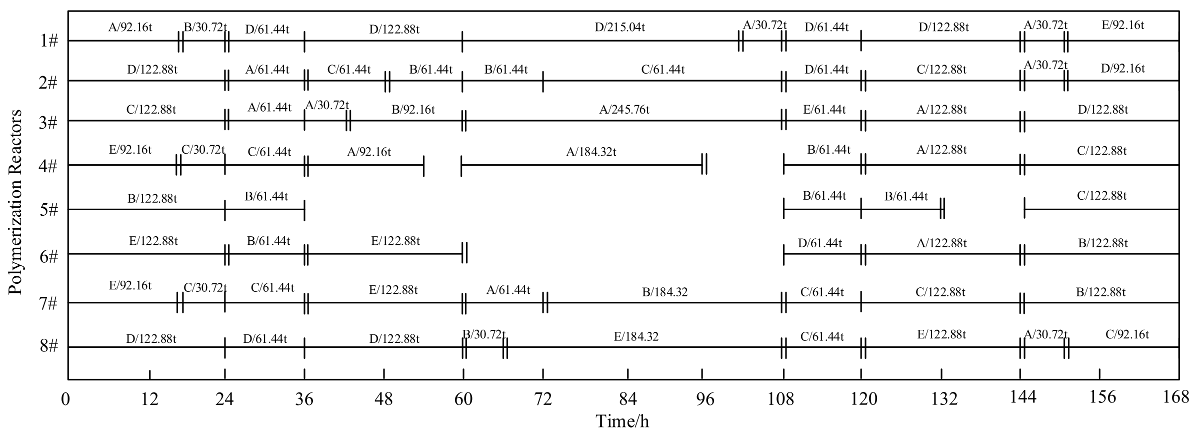

Figure 8. Scheduling of polymerization reactors of case 1.

III) is slightly less than the MINLP II because some of optimizable variables in the original MINLP model such as switch variables of equipment can be simplified by the solution of the MILP model.

Table 4 shows the objective value and computational time of the MINLP II and the MINLP III at different optimality gaps. The relationship between the objective value and computational time is shown in Figure 7 intuitively. The blue and black lines represent the optimal solution trend of the MINLP II and MILP model as the computational time changes, respectively, while the red one represents the optimal solution trend of MINLP III. The comparison results demonstrate that the rate of convergence of the optimal solution of the proposed model based on the combined algorithm is significantly faster than that of MINLP II. Meanwhile, the objective values of two cases solved by MINLP III within the time limit are 0.6% and 2.3% less than the MINLP II, respectively. Additionally, although the MILP model has a great advantage of closing the optimality gap and quick convergence as demonstrated in case 1, the objective value is relatively high because of the inevitable error of PWL. Furthermore, the scheduling of polymerization reactors obtained by the proposed model is shown in Figure 8, the optimized process of polymerization section is relatively continuous, and all orders can be completed on time. The comparative results demonstrate that the proposed model is superior to the traditional model in terms of both the computational time and the accuracy of the solution.

Some of the tips about the application of the proposed algorithm are shared as follows. From the course of the case study, we find that the initialization of the start-stop variables of equipment is critical for subsequent global optimization, which is related to whether the solution would fall into local optimality. An efficient way is to fix binary variables such as start-stop switch variables based on the solution of the MILP model and then initialize optimizable continuous variables such as production rate of equipment and cost in the improved MINLP model.

https://doi.org/10.1021/acsomega.2c00875
ACS Omega 2022, 7, 26047−26055

Additionally, the accuracy of the MILP model affects the efficiency of the improved MINLP model to a larger extent, which is illustrated in Figure 7, the rate of convergence of the improved MINLP model and the accuracy of the MILP model in case 2 (Figure 7b) is superior to that of case 1 (Figure 7a), which is because the inevitable error of the MILP model randomly varies as the production rate in the optimization process of cases vary in size, then is propagated by the initialization of start-stop variables, and is finally reflected in the convergence rate of the improved MINLP model. Therefore, it is a valuable research direction to improve the PWL to reduce the error of the MILP model.

6. CONCLUSIONS

The PVC production process is a typical hybrid system, and the difficulty of solving speed and accuracy of the PVC plant-wide scheduling problem is addressed in this paper. This paper aims to minimize the total cost of production considering the nonlinear power consumption characteristics of equipment. The MINLP model of PVC production scheduling is established based on the continuous-time modeling method, which reduced the model scale. Then, the PWL is performed on the nonlinear term in the model, and the result of the linear model is substituted into the original MINLP model as the initial value of optimizable variables. To verify the effectiveness of the proposed method, two comparative cases originating from a real PVC plant are provided. The comparisons show that the combined algorithm can significantly accelerate the solving speed. Moreover, the solution obtained from the improved model outperforms than that from the original MINLP model and MILP model. Furthermore, as a general strategy, the proposed algorithm is applicable for other similar process industry scheduling problems, which contain the process nonlinearities. In the future work, the computational problem of PVC production dynamic scheduling optimization under uncertainty will be further analyzed.

AUTHOR INFORMATION

Corresponding Author

Yuhong Wang − *College of Control Science and Engineering, China University of Petroleum, Qingdao 266580, China*; Email: Y.H.Wang@upc.edu.cn

Authors

Jian Su − *College of Control Science and Engineering, China University of Petroleum, Qingdao 266580, China*; orcid.org/0000-0001-7440-9210

Xiaoyong Gao − *Department of Automation, China University of Petroleum, Beijing 102249, China*; orcid.org/0000-0002-6893-4139

Complete contact information is available at: https://pubs.acs.org/10.1021/acsomega.2c00875

Funding

This research was supported by the National Natural Science Foundation of China (No. 21706282), National Key R&D Program of China (No. 2016YFC0303703), and the Research Foundation of China University of Petroleum (Beijing) (No. 2462020BJRC004 and No. 2462020YXZZ023).

Notes

The authors declare no competing financial interest.

ABBREVIATIONS

HH = hinging hyperplanes
PVC = polyvinyl chloride
VCM = vinyl chloride monomer
MILP = mixed integer linear programming
MINLP = mixed integer nonlinear programming

NOMENCLATURE

Indices

i = products
r = raw material (coal, coke, lime, salt)
u = units (calcium carbide furnaces/electrolytic cells/polymerization reactors/CHP units)
w = events

Sets

E = electrolytic cells
EG = CHP unit
G = calcium carbide furnaces
M = polymerization pots
MP = final products (grades of PVC)
MR = raw materials (coal, coke, lime, salt)
W = Event

Parameters

CE_w = price of procurement electricity, CNY/kWh
CI_{cac2} = inventory cost of CaC_2, CNY/t
CI_i = inventory cost of product i, CNY/t
CI_r = inventory cost of raw material r, CNY/t
CI_{vcm} = inventory cost of VCM, CNY/t
CRM_r = price of raw material r, CNY/t
CF_u = cost of start-stop operation of unit u, CNY
cy = polymerization time, h
$D_{i,w}$ = market demand of product i in the event w, t
$sFS_{u,i,w}$ = feeding quantity of unit u, t
MI_{cac2}^{max} = maximum inventory capacity of CaC_2, t
MI_{cac2}^{min} = minimum inventory capacity of CaC_2, t
MI_i^{max} = maximum inventory capacity of product i, t
MI_i^{min} = minimum inventory capacity of product i, t
MI_r^{min} = minimum inventory capacity of raw material r, t
MI_r^{max} = maximum inventory capacity of raw material r, t
MI_{vcm}^{max} = maximum inventory capacity of VCM, t
$P_{cl2,u,w}^{max}$ = maximum production rate of unit u to produce Cl_2 in the event w, kg/h
$P_{cl2,u,w}^{min}$ = minimum production rate of unit u to produce Cl_2 in the event w, kg/h
$P_{cac2,u,w}^{max}$ = maximum production rate of unit u to produce CaC_2 in the event w, t/day
$P_{cac2,u,w}^{min}$ = minimum production rate of unit u to produce CaC_2 in the event w, t/day
$Pw_{u,w}^{max}$ = maximum electric power of unit u in the event w, MW
$Pw_{u,w}^{min}$ = minimum electric power of unit u in the event w, MW
Py_i = out-of-stock penalty of product i, CNY
TH = scheduling period, h
T_{min} = shortest interval between adjacent event, h
T_w = start time of event w, h
$\alpha_{u,i}$ = conversion rate of VCM to product i in unit u
β = transfer coefficient for output of C_2H_2 and consumption of CaC_2
γ = transfer coefficient for output of HCL and consumption of Cl_2
δ = transfer coefficient for output of CaC_2 and consumption of coke

https://doi.org/10.1021/acsomega.2c00875
ACS Omega 2022, 7, 26047−26055

Variables

C_1 = raw materials cost, CNY
C_2 = stockout penalty, CNY
C_3 = inventory cost, CNY
C_4 = start-stop and product switching penalty, CNY
C_5 = electricity consumption cost, CNY
$CM_{cac2,\,w}$ = CaC_2 consumption in the event w, t
$CM_{cao,\,w}$ = CaO consumption in the event w, t
$CM_{C2H2,\,w}$ = C_2H_2 consumption in the event w, t
$CM_{cl2,\,w}$ = Cl_2 consumption in the event w, t
$CM_{coal,\,w}$ = coal consumption in the event w, t
$CM_{coke,\,w}$ = coke consumption in the event w, t
$CM_{Hcl,\,w}$ = HCL consumption in the event w, t
$CM_{Nacl,\,w}$ = NaCl consumption in the event w, t
$CM_{r,\,w}$ = raw material r consumption in the event w, t
$CM_{vcm,\,w}$ = VCM consumption in the event w, t
ele_w = electricity consumption of total PVC plant in the event w, kWh
$elesp_w$ = electricity supply in the event w, kWh
$MI_{cac2,\,w}$ = inventory of CaC_2 in the event w, t
$MI_{i,\,w}$ = inventory of product i in the event w, t
$MI_{r,\,w}$ = inventory of raw material r in the event w, t
$MI_{vcm,\,w}$ = inventory of VCM in the event w, t
$P_{cac2,\,u,\,w}$ = production rate of CaC_2 in unit u in the event w, t/day
$P_{cl2,\,u,\,w}$ = production rate of Cl_2 in unit u in the event w, kg/h
$PE_{u,\,w}$ = electricity supply of unit u in the event w, kWh
$T_{cac2,\,u,\,w}$ = production time of CaC_2 in unit u in the event w, h
$T_{cl2,\,u,\,w}$ = production time of Cl_2 in unit u in the event w, h
$T_{CHP,\,u,\,w}$ = running time of the CHP unit in the event w, h
$T_{cac2,\,u,\,w}$ = production time of unit u in the event w, h
$PT_{cac2,\,w}$ = production of CaC_2 in the event w, t
$PT_{C2H2,\,w}$ = production of C_2H_2 in the event w, t
$PT_{cl2,\,w}$ = production of Cl_2 in the event w, t
$PT_{i,\,u,\,w}$ = production of product i in unit u in the event w, t
$PT_{vcm,\,w}$ = production of VCM in the event w, t
$Pw_{u,\,w}$ = electric power of unit u in the event w, MW
$S_{i,\,w}$ = supply of product i in the event w, t
SG_w = electricity supply of the state grid, kWh
$SP_{r,\,w}$ = supply of raw material r in the event w, t
$\omega_{u,\,i,\,w}$ = 0−1 variable denoting whether the polymerization reactor u products i at event w
$y^{s}_{u,\,i,\,i',\,w}$ = 0−1 variable denoting whether polymerization reactor u starts to switch from i to i' at event w
$y^{e}_{u,\,i,\,i',\,w}$ = 0−1 variable denoting whether polymerization reactor u ends to switch from i to i' at event w
$Z_{u,\,w}$ = 0−1 variable denoting whether unit u is working in the event w
$ZF_{u,\,w}$ = 0−1 variable denoting whether unit u starts up or shuts down in the event w

REFERENCES

(1) Wang, Y.; Lian, X.; Gao, X.; Feng, Z.; Huang, D.; Chen, T.; Liu, S.; Bai, J. X. Multiperiod Planning of a PVC Plant for the Optimization of Process Operation and Energy Consumption: An MINLP Approach. *Ind. Eng. Chem. Res.* **2016**, *58*, 12430−12443.

(2) Gao, X.; Feng, Z.; Wang, Y.; Huang, X.; Huang, D.; Chen, T.; Lian, X. Piecewise Linear Approximation based MILP Method for PVC Plant Planning Optimization. *Ind. Eng. Chem. Res.* **2018**, *57*, 1233−1244.

(3) Tian, M.; Gao, X.; Jiang, Y.; Wang, L.; Huang, D. Plantwide Scheduling Model for the Typical Polyvinyl chloride Production by Calcium Carbide Method. *Ind. Eng. Chem. Res.* **2016**, *55*, 6161−6174.

(4) Tian, M.; Jiang, Y.; Huang, D. Integrated scheduling for polyvinyl chloride productive processes. *CIESC J.* **2015**, *66*, 251−258.

(5) Tian, M.; Gao, X.; Huang, D.; Jiang, Y. Inventory pinch analysis based bi-level heuristic algorithm for scheduling of the PVC production by calcium carbide method. *IEEE* **2016**, 2678−2684.

(6) Tian, M.; Gao, X.; Jiang, Y.; Huang, D.; Wang, L. A Decomposition Algorithm for the Scheduling of Typical Polyvinyl Chloride Production by Calcium Carbide Method. *Ind. Eng. Chem. Res.* **2016**, *55*, 12256−12267.

(7) Chen, G.; Yan, L.; Shi, B. Modeling and Optimization for Short-term Scheduling of Multipurpose Batch Plants. *Chin. J. Chem. Eng.* **2014**, *22*, 682−689.

(8) Floudas, C. A.; Lin, X. Continuous-time versus discrete-time approaches for scheduling of chemical processes: a review. *Comput. Chem. Eng.* **2004**, *28*, 2109−2129.

(9) Yee, K. L.; Shah, N. Improving the efficiency of discrete time scheduling formulation. *Comput. Chem. Eng.* **1998**, *22*, S403−S410.

(10) González-González, J. M.; Vázquez-Méndez, M. E.; Diéguez-Aranda, U. Multi-objective models for the forest harvest scheduling problem in a continuous-time framework. *For. Policy Econ.* **2022**, No. 102687.

(11) Christian, N.; Arild, H.; Bosong, L.; Masood, P.; Hossein, F.; Joao, P. S. C. Hydrothermal scheduling in the continuous-time framework. *Electr. Power Syst. Res.* **2020**, No. 106787.

(12) Feleke, B.; Debashish, P.; Manojkumar, R. Continuous Time Scheduling of Gasoline Production and Distribution with a Remarkable Formulation Size Reduction using Extended Graphical Genetic Algorithm. *Chem. Eng. Res. Des.* **2020**, *164*, 385−399.

(13) Jaffal, Y.; Nasser, Y.; Corre, Y.; Lostanlen, Y. K-best branch and bound technique for the MINLP resource allocation in multi-user OFDM systems. *International Workshop on Signal Processing Advances in Wireless Communications*, IEEE. 2015, 161−165.

(14) Xiang, W.; Kanjian, Z.; Ming, C. A gradient-based algorithm for non-smooth constrained optimization problems governed by discrete-time nonlinear equations with application to long-term hydrothermal optimal scheduling control. *J. Comput. Appl. Math.* **2022**, *412*, No. 114335.

(15) Jodie, M. S.; Michael, B. Parameterizations of data-driven nonlinear dynamic process models for fast scheduling calculations. *Comput. Chem. Eng.* **2019**, 106498.

(16) Zhen, G. A. O.; Lixin, T. A. N. G.; Hui, J. I. N.; Nannan, X. U. An Optimization Model for the Production Planning of Overall Refinery. *Chin. J. Chem. Eng.* **2008**, *16*, 67−70.

(17) Yamin, W.; Xia, Z.; Qihui, J. Establishment and Application of Production Planning Optimization Model in Coking & Chemical Enterprises. *Process Autom. Instrum.* **2008**, *29*, 72−75.

(18) You, F.; Grossmann, I. E. Integrated multi-echelon supply chain design with inventories under uncertainty: MINLP models, computational strategies. *AIChE J.* **2009**, *56*, 419−440.

(19) Xu, J.; van den Boom, T. J.; De Schutter, B.; Wang, S. Irredundant lattice representations of continuous piecewise affine functions. *Automatica* **2016**, *70*, 109−120.

(20) Xu, J.; van den Boom, T. J.; De Schutter, B.; Luo, X. L. Minimal Conjunctive Normal Expression of Continuous Piecewise Affine Functions. *IEEE Trans. Autom. Control* **2016**, *61*, 1340−1345.

https://doi.org/10.1021/acsomega.2c00875
ACS Omega 2022, 7, 26047−26055